Pteridine-based fluorescent pH sensors designed for physiological applications

ARTICLE *in* JOURNAL OF PHOTOCHEMISTRY AND PHOTOBIOLOGY A CHEMISTRY · NOVEMBER 2012

Impact Factor: 2.5 · DOI: 10.1016/j.jphotochem.2012.08.002

6 AUTHORS, INCLUDING:

John P. Graham
United Arab Emirates University
41 PUBLICATIONS **122** CITATIONS
SEE PROFILE

Akef Afaneh
University of Manitoba
7 PUBLICATIONS **19** CITATIONS
SEE PROFILE

Yaseen A. Al-Soud
Al - Albayt University
103 PUBLICATIONS **1,157** CITATIONS
SEE PROFILE

Fatima Esmadi
Yarmouk University
23 PUBLICATIONS **210** CITATIONS
SEE PROFILE

Journal of Photochemistry and Photobiology A: Chemistry 247 (2012) 63–73

Contents lists available at SciVerse ScienceDirect

Journal of Photochemistry and Photobiology A: Chemistry

journal homepage: www.elsevier.com/locate/jphotochem

Pteridine-based fluorescent pH sensors designed for physiological applications

Na'il Saleh[a,d,*], John Graham[a], Akef Afaneh[b], Yaseen A. Al-Soud[c], Georg Schreckenbach[b], Fatima T. Esmadi[d]

[a] Department of Chemistry, College of Science, United Arab Emirates University, P.O. Box 17551, Al-Ain, United Arab Emirates
[b] Department of Chemistry, University of Manitoba, Winnipeg, MB R3T 2N2, Canada
[c] Department of Chemistry, Faculty of Science, University of Al al-Bayt, Al-Mafraq, Jordan
[d] Department of Chemistry, Faculty of Science, Yarmouk University, Irbid, Jordan

ARTICLE INFO

Article history:
Received 16 May 2012
Received in revised form 25 July 2012
Accepted 7 August 2012
Available online xxx

Keywords:
Pteridine
Fluorescent pH sensors
Protonation/deprotonation
DFT calculations
Physiological pH

ABSTRACT

New derivatives of pteridine, namely 6,7-diphenyl-2-morpholinylpterin (**DMPT**) and 6-thienyllumazine (**TLM**) were designed and easily synthesized in a rational way for pH-fluorescence sensing near physiological pH. The dual-excitation ratiometric sensing was based on the distinct spectral properties of the fluorophore in its neutral and deprotonated states. Density Functional Theory (DFT) calculations were used to determine structures, gas phase acidities and pK_a values for the new dyes. Substitutions on pterin (**PT**) and lumazine (**LM**) structures with phenyl, thienyl or morpholinyl groups enhanced the acidity of the new dyes. **DMPT** displays visible turn-on emission signals from blue to cyan (bluish-green) upon changing the pH from acidic to basic around pK_a of 7.2. The advantages of the new pteridine dyes over those previously known pH sensors are discussed in details in terms of their facile preparation and functionalization, pK_a tuning strategy, wide responsive and resolved signal around physiological pH, photostability, water solubility, and adequacy for intracellular pH measurements.

1. Introduction

Continuous, real-time monitoring of pH in a nondestructive, reversible way with high sensitivity and selectivity can be performed by using small organic molecules with emissive properties in aqueous solutions [1–5]. Such molecular tools, which are known as fluorescent sensors have already been designed and synthesized by many researchers for sensing applications that are relevant to environment [6,7], biology [8], and nanotechnology [9]. In some applications related to food [10] and forensic sciences [11], the rapid, simple (mostly visible) fluorescence signaling becomes advantageous as it reduces the need for labor intensive, time-consuming, and expensive techniques.

Several fluorophores were reported in literature to display pH-dependence absorption and fluorescence spectra in a range around their ground- and excited-state pK_a, respectively. The pH-responsive properties have not only been examined for small molecules in solutions, but also for complexed media such as polymeric hydrogels [12], polymeric dendimers [13], fiber optic [14], and nanoparticles [15]. In many occasions, the optical changes were based on photoinduced proton transfers, photoinduced electron transfers (PET) [16–20], foster resonance energy-transfers (FRET) [21], or intramolecular charge transfers (ICT) [22].

Many molecular fluorescent sensors with modulated pK_a near-neutral pH were designed with the purpose of monitoring pH changes inside living cells [8]. Examples, just to name few, include those dyes based on carboxyfluorescein (BCPCF) (pK_a 7.0) [23], seminaphthofluorones (SNARFs) (pK_a 7.2) [24], cyanine dyes (pK_a 7.2) [25], rhodamines (pK_a 6.5) [26], and 1,8-naphthalimide (pK_a 7.4) [19].

In recent years, we have become interested in pursuing the fluorescence properties in aqueous solutions of new derivatives of lumazine (2,4-dihydroxypteridine) (**LM**) and pterin (2-amino-4-hydroxypteridine) (**PT**) heterocyclic natural compounds that are soluble in water [27,28]. The compounds investigated in the present study are 6-thienyllumazine (**TLM**) (see Fig. 1) and 6,7-diphenyl-2-morpholinylpterin (**DMPT**) (see Fig. 2). The pteridine substrates (**PT** and **LM**) are generally known for their importance in biological systems (e.g., folic acid) [29] and interesting photochemical and photobiological properties [30,31], thus the photochemistry and photophysics of this family of compounds have been the subject of several reports in many occasions [32–36]. From another prospective, the acyl urea moiety in **LM** was easily functionalized to crown ether [37]. Also, the **LM** was used as a platform for metal ion sensing by us and others [27,28,38]. In the course of our study on the fluorescence sensing/chelating properties of **TLM** against heavy toxic metal ions such as cadmium and mercury, we noticed that the absorption and fluorescence spectral profiles of the dye were

* Corresponding author at: Department of Chemistry, College of Science, United Arab Emirates University, P.O. Box 17551, Al-Ain, United Arab Emirates.
Tel.: +971 3 713 6138.
E-mail address: n.saleh@uaeu.ac.ae (N. Saleh).

1010-6030/$ – see front matter © 2012 Elsevier B.V. All rights reserved.
http://dx.doi.org/10.1016/j.jphotochem.2012.08.002

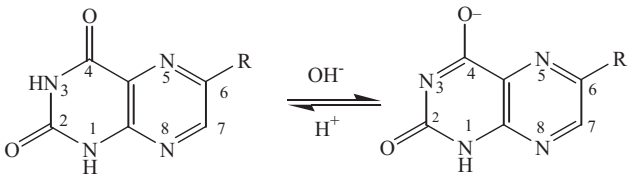

R	Compound
-H	Lumazine (**LM**)
- Thiophene	6-Thienyllumazine (**TLM**)

Fig. 1. The molecular structures of **TLM** and its parent molecule (**LM**), as well as the acid - base equilibrium in aqueous solutions in the pH range 4–10.

highly dependent on pH values of the media. More importantly, it was concluded [27] that the addition of thiophene stabilizing group lowered the pK_a value in the ground and excited states of the lumazine platform into neutral pH (from ca. 7.9 [39–43] to ca. 6.8 see Section 3).

In view of these findings, we have designed **DMPT**, in which two phenyl and one morpholine were introduced to the pterin platforms with the goal of tuning the pK_a value into a physiological pH (ca. 7.2, see Section 3) through the stabilization of the conjugate base. Putting it all together, we present herein two pH fluorescent sensors for biological imaging applications, namely **DMPT** and **TLM**, whose pK_a values come near-neutral pH values. The new dyes are more photostable, water soluble, and much easily prepared when compared to other known fluorescent pH indicators [8]. Theoretical investigations of the two pteridine-based dyes **TLM** and **DMPT** were also conducted to demonstrate the enhancement of their acidity when compared to that of the parent molecules.

2. Experimental

2.1. Materials

All starting materials and solvents were of spectroscopic grades and used as purchased from Sigma–Aldrich. Millipore water was used for the measurement.

2.2. Methods

2.2.1. Instruments and optical spectroscopic measurements

^{1}H NMR and ^{13}C NMR spectra in DMSO-d_6 were recorded at 250 MHz (^{1}H) and at 150.91 MHz (^{13}C) with a Bruker DPX-300 spectrometer (Bruker, Germany) and are reported in ppm (δ) relative to TMS as an internal standard. EIMS spectra were obtained using a Finnegan FAB MAT 8200 spectrometer (Finnigan MAT, USA) at 70 eV. Elemental analyses were acquired with the aid of a Vario Elementar apparatus (Shimadzu). Melting points were measured on a B-545 Büchi melting point apparatus (Büchi Labortechnik AG, Switzerland) and are uncorrected. The UV–vis absorption spectra were measured on Cary-50 instrument (Varian). The pH values of the solutions were adjusted (±0.2 units) by adding adequate amounts of HCl or NaOH and recorded using a pH meter (WTW 330i equipped with a WTW SenTix Mic glass electrode). Fluorescence spectra were measured using Cary-Eclipse instrument with a slit width of 5 nm for the excitation monochromator in any measurements, while a slit width of 2.5 nm and 5 nm were used for the emission monochromator in the measurement of the fluorescence spectra of **TLM** and **DMPT**, respectively. The wavelengths 368 nm and 372 nm were selected for the emission measurement of **TLM** and **DMPT**, respectively, being the isosbestic points in the absorption spectra against pH. The fluorescence quantum yields were

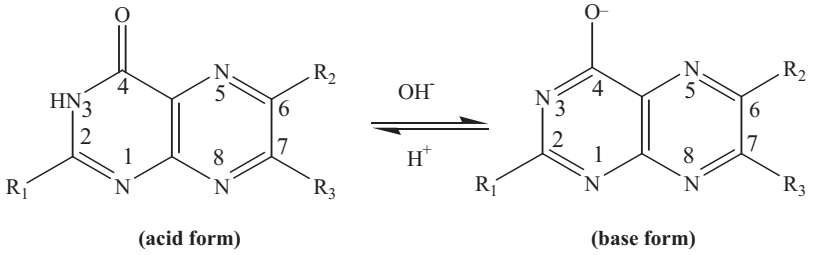

R_1	R_2	R_3	Compound
-NH_2	-H	-H	pterin (**PT**)
	-H	-phenyl	7-phenylpterin (**PPT**)
- morpholine	-H	-H	2-morpholinylpterin (**MPT**)
-NH_2	-phenyl	-phenyl	6,7-diphenylpterin (**DPT**)
- morpholine	-phenyl	-phenyl	6,7-diphenyl-2-morpholinylpterin (**DMPT**)

Fig. 2. The structures of different derivatives based on pterin and the acid–base equilibrium in aqueous solutions in the pH range 4–10. Only **DMPT** was synthesized in the present study.

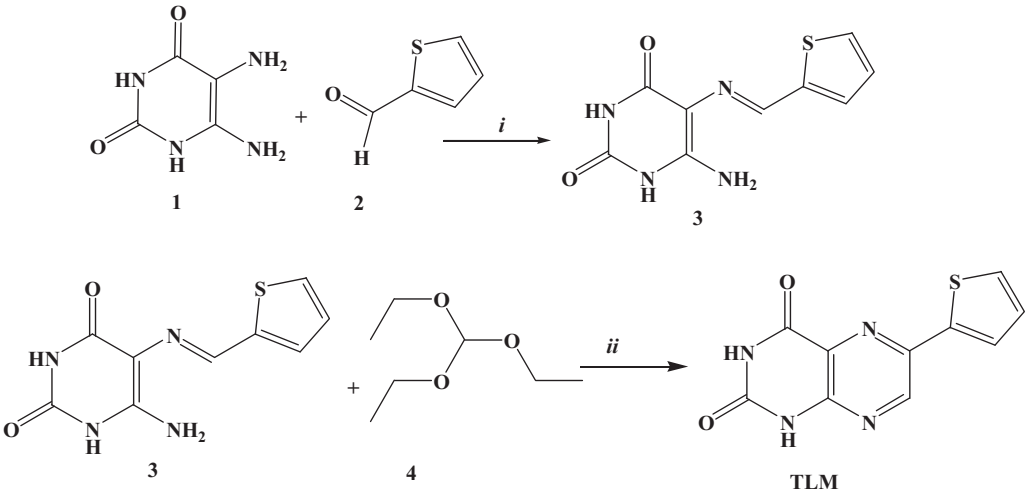

Fig. 3. Reagent and conditions: (i) DMF, reflux, 4 h; (ii) DMF, reflux, 10 h.

determined with coumarin 2 (**C450**) in acetonitrile as the standard (Φ = 0.8) [44] using the known equation, Eq. (1) [1]:

$$\phi_{unk} = \phi_{std}\left(\frac{I_{unk}}{A_{unk}}\right)\left(\frac{A_{std}}{I_{std}}\right)\left(\frac{n_{unk}}{n_{std}}\right)^2 \quad (1)$$

The excitation-dependence fluorescence spectra for **DMPT** were remained unchanged, suggesting that only one excited state (fluorophore) contributed to the observed fluorescence in agreement with a previous report for pterin compounds [32]. The emission wavelength for the excitation spectra measurements of **DMPT** (e.g., 472 nm) were selected as the intersected point between the emission spectra of the acidic and basic forms. For **TLM**, the excitation spectra were monitored at the emission maxima 452 nm of both the acidic and basic species, as previously reported by us [27,28].

2.2.2. pK_a determination by sigmoidal fitting

The pK_a value was determined from the sigmoidal fitting available in SigmaPlot software for both the UV–vis absorption and fluorescence titration data at the indicated wavelength in the Supporting Information, using the following expression, Eq. (2) [45]:

$$Y^{\lambda}_{obs} = \frac{Y^{\lambda}_{A}}{1+10^{pH-pK_a}} + \frac{Y^{\lambda}_{A^-}}{1+10^{pK_a-pH}} \quad (2)$$

where $Y(\lambda)$ is the observed absorbance or fluorescence intensities at a given λ. $Y_A(\lambda)$ is the absorbance or fluorescence intensities of the acidic form alone at the selected wavelength λ. $Y_{A^-}(\lambda)$ is the absorbance or fluorescence intensities of the basic form alone at the selected wavelength λ.

For the ratio of the excitation intensities at two selected wavelengths, the following expression was inserted to the SigmaPlot program to fit the observed data:

$$\frac{Y_{\lambda_1}}{Y_{\lambda_2}} = \frac{Y^{\lambda_1}_{A}/Y^{\lambda_2}_{A}}{1+(Y^{\lambda_2}_{A^-}/Y^{\lambda_2}_{A})10^{pH-pK_a}} + \frac{Y^{\lambda_1}_{A^-}/Y^{\lambda_2}_{A^-}}{1+(Y^{\lambda_2}_{A}/Y^{\lambda_2}_{A^-})10^{pK_a-pH}} \quad (3)$$

where $Y(\lambda_1)/Y(\lambda_2)$ is the ratio of the observed excitation intensities at two emission wavelengths λ_1 and λ_2. $Y_A(\lambda_2)$ is the intensity of the acidic form alone at the second emission wavelength (λ_2). $Y_{A^-}(\lambda_2)$ is the intensity of the basic form alone at the second emission wavelength (λ_2). $Y_A(\lambda_1)$ is the intensity of the acidic form alone at the first emission wavelength (λ_1). $Y_{A^-}(\lambda_1)$ is the intensity of the basic form alone at the first emission wavelength (λ_1). All of these initial values were left as floating parameters in the analysis by Levenberg–Marquardt algorithm, which was provided by the SigmaPlot's software (version 6.1; SPCC, Inc., Chicago, IL, USA).

2.3. Synthesis of 6-thienyllumazine (*TLM*)

6-Thienyllumazine was prepared in two steps. The first step involves reaction of 5,6-diaminouracil (**1**) with 2-thiophene carbaldehyde (**2**) in a 1:1 molar ratio to produce 5-thiophenylideneaminouracil (**3**), which was reacted further with triethylformate to produce the required compound (**TLM**), see Fig. 3.

2.3.1. Synthesis of 6-amino-5-thiophenylideneaminouracils (*3*)

A suspension of 5,6-diaminouracil (**1**) (0.06 mol) and 2-thiophene carbaldehyde (**2**) (0.06 mol) in dimethylformamide (40 ml) was refluxed for 4 h. After cooling the solution, a light yellow precipitate was formed which was filtered, washed with hot water and recrystallized from ethanol (2.06 g, 58%); decomposition temperature 256–260 °C; ^{1}H NMR (DMSO-d$_6$; 400 MHz; Me$_4$Si): δ 10.64 (br s, 1H, H-3); 10.54 (s, 1H, H-1); 9.72 (s, 1H, H—C=N); 6.42 (s, 2H, NH$_2$); 7.56 (d, 1H, H-S-1); 7.39 (d, 1H, H-S-3); 7.09 (dd, 1H-S-2); IR (cm^{-1}), KBr disk; $\nu_{C=N(imine)}$, 1650 (s); ν_{NH} (amine), 3100; Anal Calc. for $C_9H_8N_4O_2S$ (236.25): C, 45.76; H, 3.41; N, 23.71, S, 13.57. Found: C, 45.83; H, 3.51; N, 22.84; S, 13.24, *m/z*, 236.3.

2.3.2. Synthesis of 6-thienyllumazine (*TLM*)

Triethylformate (**4**) (15 g, 0.1 mol) was added to a solution of 6-amino-5-thiophenylideneamineouracil (**3**) (0.02 mol) in dimethylformamide (25 ml). The mixture was refluxed for 10 hours. Upon cooling, a yellow precipitate was formed, which was filtered and then recrystallized from dimethylformamide. Decomposition point 281–284 °C, ^{1}H NMR (DMSO-d$_6$, 400 MHz, Me$_4$Si): δ 10.60 (s, 1H, H-3); 10.53 (s, 1H, H-1), 9.72 (s, 1H, H-7); 7.57 (d, 1H, H-S-1); 7.37 (d, 1H, H-S-3); 6.91 (dd, 1H, H-S-2); IR (cm^{-1}), KBr disk; $\nu_{C=O}$, 1723, 1736, $\nu_{C=N}$, 1582. Anal. Calc. for $C_{10}H_6N_4O_2S$ (246.25): C, 48.78; H, 2.46; N, 22.75; s, 13.02. Found, C, 48.29; H, 2.56; N, 23.84; S, 12.64, *m/z* 246.3.

2.4. Synthesis of 6,7-diphenyl-2-morpholinylpterin (*DMPT*)

5,6-Diamino-2-(benzylsulfanyl)-4(3H)-pyrimidinon **6** (see Fig. 4) prepared from compound **5** reacted with benzil at room temperature afforded 2-(benzylsulfanyl)-6,7-diphenyl-4(3H)-pteridinon **7** [46]. Compound 7 (100 mg, 0.237 mmol) was dissolved in dry DMF (3.0 ml). To this solution was added m-CPBA (3.0 equiv., 1.01 mmol, 174 mg) and was stirred under nitrogen for 3 h at room temperature. The solvent was then removed under

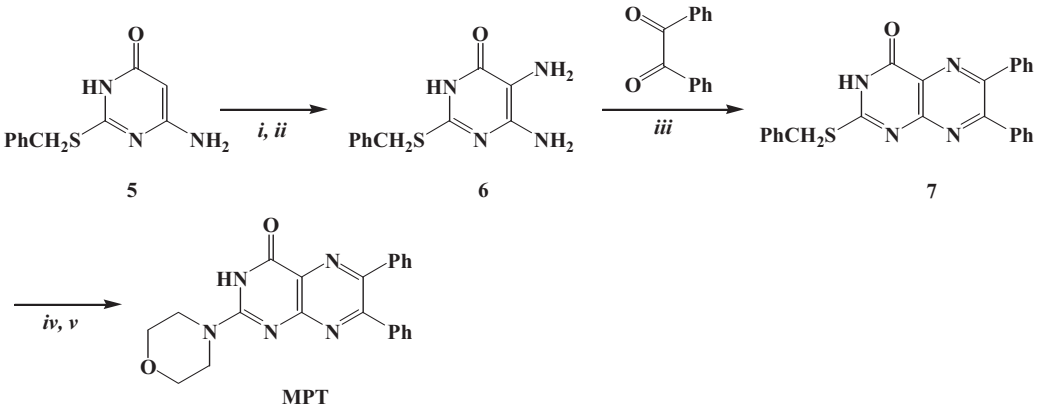

Fig. 4. Reagents and conditions: (i) HNO_2; (ii) $Na_2S_2O_4$; (iii) EtOH, reflux; (iv) DMF, m-CPBA, rt. 3 h; (v) morpholine, MW, 110 °C, 1 h.

reduced pressure and the resulting solid was dissolved in morpholine (2.0 ml, 23.12 mmol) and heated in the microwave at 110 °C for 1 h. The excess solvent was also removed under reduced pressure and the resulting residue was purified by flash chromatography to yield the title compound **DMPT** as a yellow solid (85 mg, 0.220 mmol, 93%), mp >210 °C. ^{1}H NMR (DMSO-d_6): δ 3.70–3.72 (m, 8H, morpholine-H); δ 7.33–7.43 (m, 10H, ArH); δ 11.87 (bs, 1H, NH). ^{13}C NMR (DMSO-d_6): δ 45.17 (2× CH_2, C-morpholine), 65.62 (2× CH_2, C-morpholine), 126.54, 128.02, 128.06, 128. 22, 129.16, 129.42, 129.58, 138.17, 138.31, 147.22, 152.38, 156.81, 156.85, 161.67. LC/MS calcd for $C_{22}H_{19}N_5O_2$ $[M+H]^+$, 385; found, 386. Anal. calc. for $C_{22}H_{19}N_5O_2$: C, 68.56; H, 4.97; N, 18.17. Found: C, 68.41; H, 4.86; N, 18.31.

2.5. Computational details

All calculations were performed using Gaussian 03 [47]. Energy minima were determined without symmetry constraints and verified by vibrational frequency calculations. The B3LYP hybrid functional [48] and 6-311G+(d,p) basis set were used for geometry optimization and frequency calculations. The CPCM model [49] was used to model H_2O in calculation of solvation energies.

3. Results and discussion

3.1. Photophysical properties in aqueous and organic solvents

Table 1 summarizes the photophysical properties of **DMPT** at 25 °C in several organic solvents and in water at different pH values. Similar to the spectroscopic results reported for **TLM** [27], the initial observation of this table established that the polarity and viscosity of the media have no influence on the spectroscopic properties of **DMPT** (e.g., optical peak positions or intensities). As an example, the polarity and polarizability parameters (π^*) [50] were tested and could not correlate with the fluorescence or absorption maxima. Nevertheless, absorption and fluorescence maxima change only slightly with solvents variations. While, the absorption and emission peak maxima of **DMPT** in comparison with those observed for **PT** look very similar in the pH range from 4 to 10 (only red-shifted), the estimated quantum yields are different [32–34], probably because (i) the larger substituents of the studied compounds in this work act as an internal quencher, as in the case of folic acid [51]; (ii) other compounds present in the solutions quench the fluorescence. It has been reported that anions and organic compounds are able to act as fluorescence quenchers of pterins [52,53]. As an initial test, the photolysis of **DMPT** in aqueous solutions upon irradiations with a UVB lamp of 300 nm and a power of 12 mW/cm^2 was investigated and the initial observation (see Fig. S1 in the Supporting Information) indicated that the dye is more stable than **C450** by a factor of 2-fold. Nevertheless, the plan in the future is to study the photostability of this group of dyes in details and under the conditions used in real cellular imaging.

3.2. pH-dependent change of the UV–vis absorption and the fluorescence spectra

Graphs from Figs. S2–S14 in the Supporting Information illustrate the change in the absorption and fluorescence spectra as a

Table 1
The spectral characteristics and the emission quantum yields of **DMPT** (10 μM) in different solvents [62].

Solvent	Solvent parameters			Absorption		Emission	
	ε[a]	η[b]	π^*[c]	λ_{max} (nm)	ε (l cm^{-1} mol^{-1})[d]	λ_{max} (nm)	Φ_F[e]
1,4-Dioxane	2.27	1.2	0.55	380	6740	457	0.06
Ethanol	24.6	1.1	0.54	380	9250	463	0.09
Acetonitrile	35.94	0.35	0.75	380	8540	459	0.08
Ethylene glycol	37.7	16.1	0.92	384	9650	471	0.1
Dimethyl sulfoxide (DMSO)	46.71	2.1	1.00	386	12,140	470	0.08
Water (pH = 1.0)	78.3	0.89	1.09	375	10,357	460	0.02
Water (pH = 3.0)	78.3	0.89	1.09	380	12,048	472	0.06
Water (pH = 7.0)	78.3	0.89	1.09	382	12,384	475	0.06
Water (pH = 12.0)	78.3	0.89	1.09	396	13,645	486	0.04

[a] Solvent dielectric constants at room temperature.
[b] Solvent viscosities in centipoises at room temperature.
[c] Solvent polarity and polarizability according to Taft and Kamlet at room temperature [50].
[d] The most red-shifted absorption of the lumazine chromophore.
[e] Measured using coumarin 2 (**C450**) in acetonitrile as the standard (Φ = 0.8) [44], and calculated using the known equation, Eq. (1) [1]:

$$\phi_{unk} = \phi_{std}\left(\frac{I_{unk}}{A_{unk}}\right)\left(\frac{A_{std}}{I_{std}}\right)\left(\frac{n_{unk}}{n_{std}}\right)^2.$$

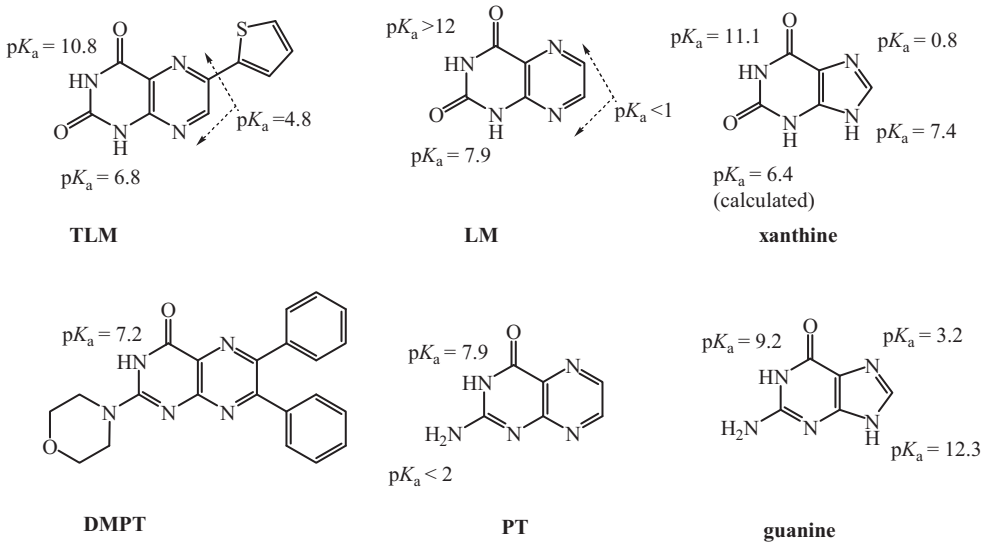

Fig. 5. The assignment of the experimental pK_a values near neutral pH (6.8 for **TLM** and 7.2 for **DMPT**) in the ground state was supported by the reported data for related compounds such as **LM** [39–43], **PT** [32], as well as **guanine** and **xanthine** [55,56].

function of pH values for the two dyes. The observed optical data in each of the corresponding figure were fitted to Eq. (2), with the goal of calculating the pK_a values for the relevant acid–base equilibrium in the ground and excited states in the pH range from 1 to 13.

Fig. 5 summarizes the previous assignments of the pK_a values observed in the ground states for related compounds such as **LM** [27,33,39–43,54], **PT** [32] as well as **xanthine** and **guanine** [55,56]. Consequently, three pK_a values were confirmed to exist from the changes in the absorption profiles of **TLM** in the pH range from 1 to 13: (i) pK_a = 4.8 attributed to the protonation of the pyrazine moiety in **TLM**, (ii) pK_a = 6.8 associated with the optical changes due to the deprotonation process of the neutral molecule that produced the monanion form, and (iii) pK_a = 10.8 attributed to the deprotonation process from the monanion form to the dianion form. The fluorescence pH titration data produced a much lower pK_a for the first acid–base equilibrium in the excited state than in the ground state (pK_a* = 2.3), indicating that **TLM** becomes more acidic in its excited state through a photoinduced proton transfer mechanism (i.e., undergoes deprotonation upon excitation). However, the value of the second pK_a from the fluorescence data has remained unchanged (pK_a* = 6.7), which implies absence of proton transfer upon excitation due to the immediate deactivation of the excited acid (base) state. For **DMPT** in the pH range from 1 to 4, pK_a of 0.95 and pK_a* of 1.8 were observed in the ground and excited states, respectively, which were attributed to the inserted morpholine group. The second pK_a in the ground and excited state occurred at 7.2 and was attributed to the deprotonation process of amide group (acid form) to phenolate group (base form) (see Fig. 2).

Table 2 summarizes the decrease in the second pK_a values (the most important pK_a to biomedical applications being closer to the physiological pH) due to the substitutions of phenyl, morpholinyl, and thienyl groups in the structures of **PT** and **LM**. Notice that this pK_a was tuned from 7.9 (in **PT**) to 7.2 (in **DMPT**), which should enabled pH sensing within a wider variation around the physiological value in cellular imaging.

It is seen from the spectra in Figs. 6 and 7 that **TLM** and **DMPT** pH indicators allow ratiometric measurements of the excitation intensities corresponding to the dual-excitation wavelengths 380/358 nm and 400/450 nm, respectively. The corresponding calibration curve was fitted to Eq. (4) (or Eq. (3) in Section 2) [1]:

$$\mathrm{pH} = \mathrm{p}K_a + \log\frac{R - R_A}{R_B - R} + \log\frac{Y_A(\lambda_2)}{Y_B(\lambda_2)} \quad (4)$$

where R is the ratio $Y(\lambda_1)/Y(\lambda_2)$ of the excitation intensities at two excitation wavelengths λ_1 and λ_2. The fitting process gave pK_a value of 6.8 and 7.2 (see Fig. 8) for **TLM** and **DMPT**, respectively, in pure water at room temperature in agreement with those obtained from the absorption and fluorescence pH-titration data in the pH range from 4 to 10.

3.3. Computational characterization of *TLM* and *DMPT*

3.3.1. Structure

Geometry optimization calculations for **TLM** identified two planar energy minima corresponding to cis- and trans-isomers, as shown in Fig. 9. The planarity of both energy minima suggests the presence of resonance between the thiophene ring and lumazine moiety. The linking carbon atoms between the two ring systems exhibit a bond length of 1.453 Å (1.457 Å in trans-isomer), shorter than the value of 1.477 Å given by others for two trigonally linked sp^2 carbon atoms [57]. Furthermore, the bond order between the linking carbon atoms calculated by natural population analysis is 1.1, indicative of some π-bonding between the two atoms. Hence the planar geometry is proposed to arise due to π-delocalization across the two ring systems, consistent with the results of Hartree–Fock calculations previously published by Saleh et al. [27]. Comparison of bond lengths in **LM** and **TLM** (Fig. 9), coupled with the relatively small enhancement in bond order described above, suggest that resonance, while sufficient to favor a planar

Table 2
The experimental and calculated pK_a values for the pteridines-based dyes, HOMO energy of the conjugate base, and ΔG (kcal/mol) for the process $HA_{(g)} \rightleftharpoons H^+_{(g)} + A^-_{(g)}$ in the gas phase.

	pK_a (expt.)	pK_a (calc.)	ΔG (g)	Anion HOMO (eV)
LM	7.9[b]	10.8	322.2	−2.29
TLM	6.8[a]	11.5	319.8	−2.34
PT	7.9[c]	12.3	322.2	−2.09
DMPT	7.2[a]	8.6	317.8	−2.41
MPT	–	–	–	−2.23
DPT	–	–	–	−2.31

[a] The experimental pK_a values determined from the spectrophotometric titration in the pH range from 4 to 10, cf. Figs. 6 and 7; error ±1%.
[b] Literature values obtained from spectrophotometric titration [39–42].
[c] Literature values obtained from spectrophotometric titration [32].

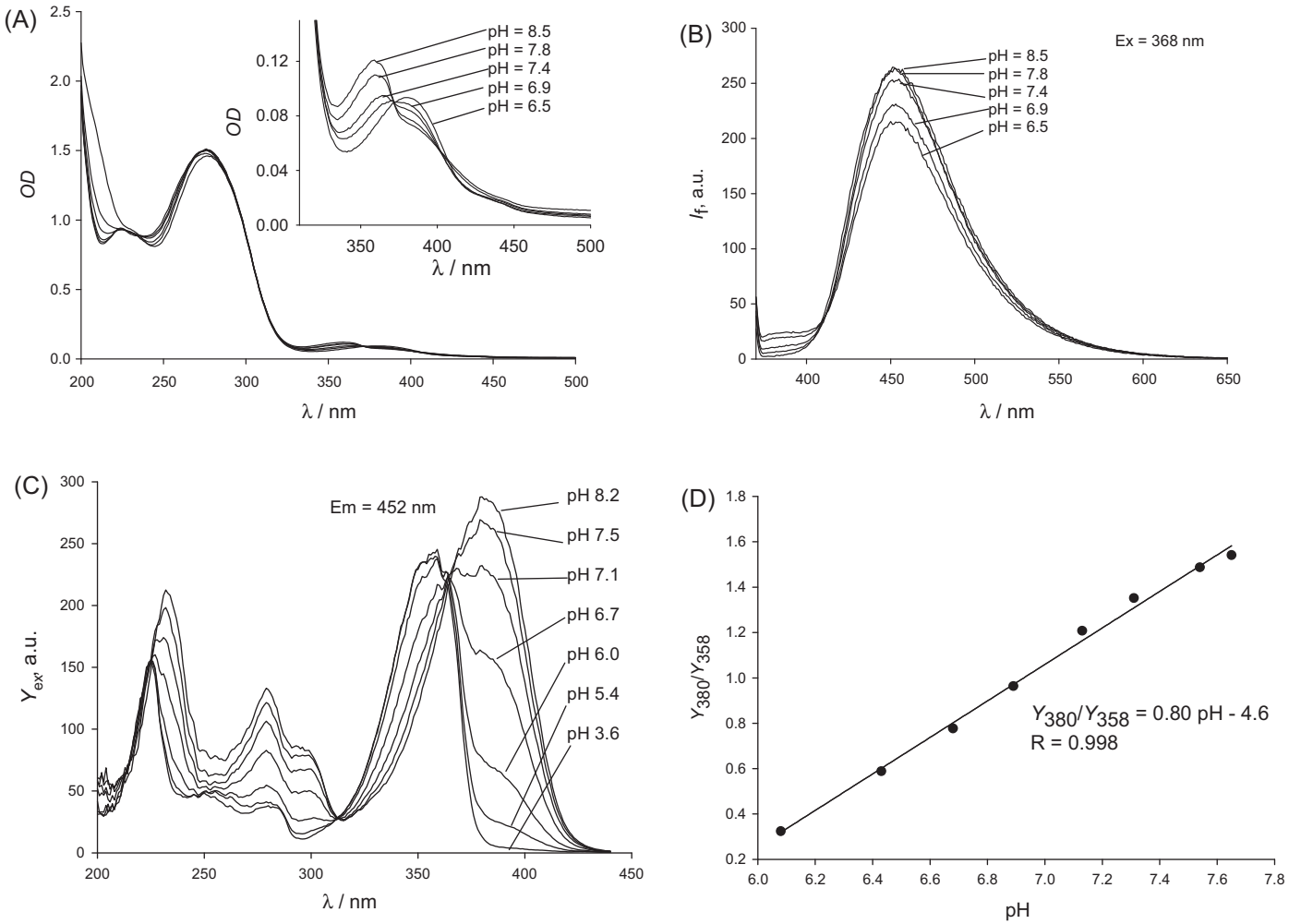

Fig. 6. The pH-dependent spectra of **TLM** (215 μM) in the pH range from 4 to 10: (A) absorption spectra (pK_a = 6.84 ± 0.07), (B) fluorescence spectra (pK_a = 6.72 ± 0.07), (C) excitation spectra (pK_a = 6.61 ± 0.02), and (D) the dual-excitation ratiometric response (Y_{350}/Y_{380}) with the linear fitting to changing the pH value (from 6.0 to 7.7), monitored at 452 nm.

geometry, is not otherwise especially strong. Consequently, the influence of resonance on the acidity of the system may be limited.

The optimized structure of **DMPT** is given in Fig. 10. Due to steric interactions, the phenyl groups cannot be co-planar with the pterin ring structure, and adopt a propeller like confirmation with dihedral angles of approximately 40°. The C—C bond lengths linking the phenyl groups to the pyrazine ring are calculated to be 1.488 Å, consistent with σ-only bonding between the sp^2 hybridized carbon atoms. The bond order between the linking C atoms is calculated to be 1.0, also consistent with a lack of resonance. There is some small distortion from planarity observed in the pyrazine ring also, illustrated in the side-on view of Fig. 10(B). Calculations on the **PPT**, with only one phenyl group, indicate that the steric interactions are reduced, but co-planarity with the pterin rings system is still inhibited due to repulsion between the phenyl group and pyrazine H (—CH). The dihedral angle between phenyl ring and pyrazine ring in **PPT** is reduced to 15° and no distortion is observed in the planarity of the pyrazine ring.

3.3.2. Acidity

To model the acid–base behavior of **TLM** and **DMPT**, calculations of pK_a values and gas-phase acidities were performed. Other properties such as charge distributions and orbital energies were also examined. In the case of **TLM**, it was determined that the proton on N1 (see Fig. 1) is considerably more acidic than that on N3 (a difference of ~7–8 kcal/mole in gas phase acidity). Consequently, the discussion below focuses on calculations involving deprotonation of N1 of **TLM**.

Calculation of pK_a values were performed following Scheme 1 of Ref. [58], in which solvation energies were calculated by the CPCM method [49] and the values −6.28 kcal/mole and −265.9 kcal/mole were used for $G_g(H^+)$ and $\Delta G_s(H^+)$ respectively [59,60]. The calculated pK_a values are summarized in Table 2. The calculations in each case overestimated the values of pK_a, with errors ranging from 1.4 to 4.7 units. The poor agreement of calculated and experimental pK_a values most likely reflects errors in calculated solvation energies using the continuum model. Calculations using explicit solvation models might improve the accuracy of pK_a values, but would be prohibitively expensive for large systems such as these.

The calculated gas phase acidities, defined as ΔG (kcal/mol) for the process $HA_{(g)} \rightleftharpoons H^+_{(g)} + A^-_{(g)}$ show better correlation with the experimental data. The gas phase acidity of **DMPT** is calculated to be 4.4 kcal/mol higher than that of **PT** and that of **TLM** 2.4 kcal/mol higher than that of **LM**. In each case, the substituted compound is predicted to be inherently more acidic than the parent molecule, consistent with the experimentally determined pK_a (see also Table 2). However, a quantitative relationship is not expected or observed in the absence solvation effects.

Examination of charge distributions, in particular the positive charge on the ionizable proton calculated by natural population

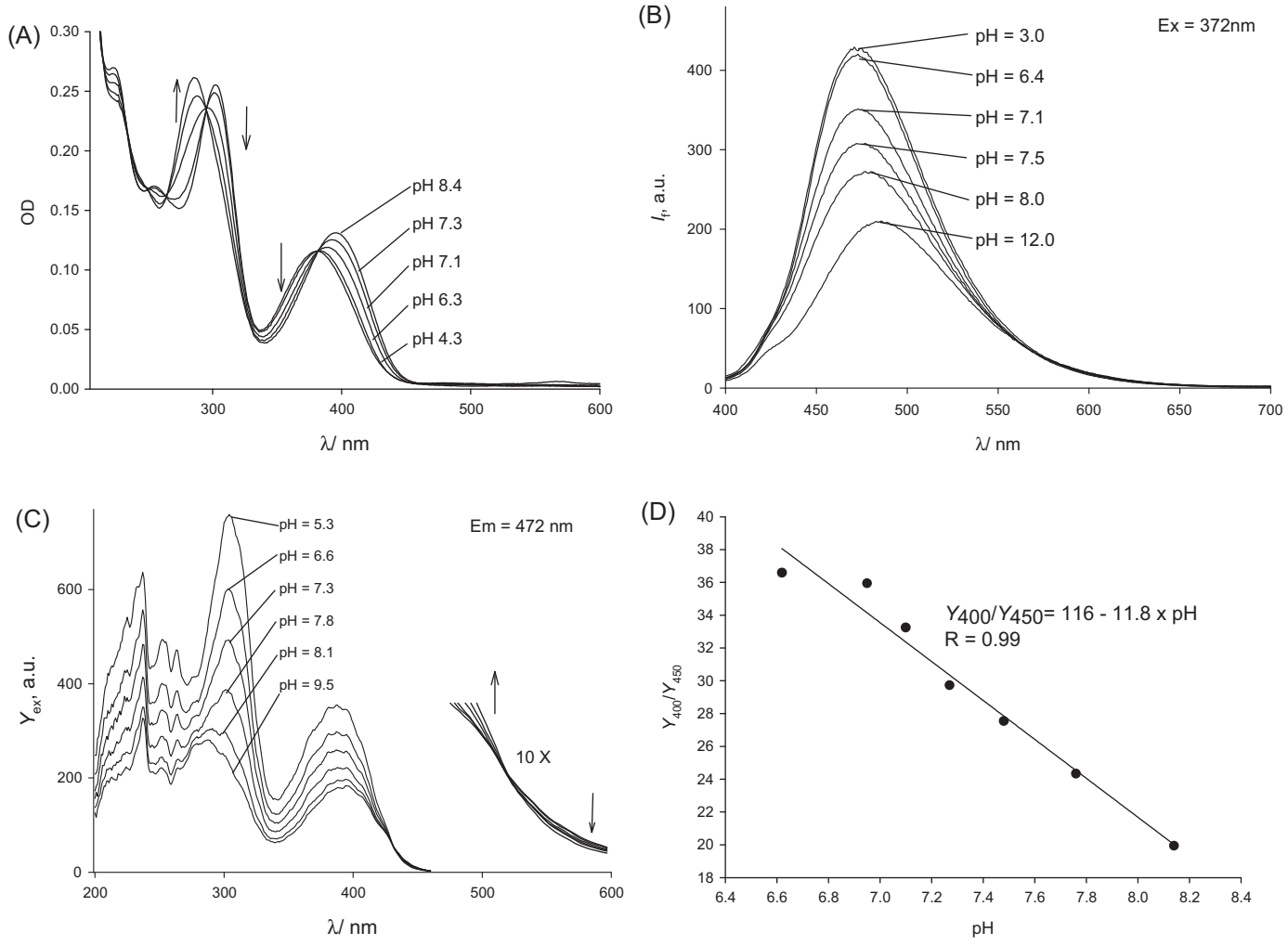

Fig. 7. The pH-dependent spectra of **DMPT** (10 μM and 4 μM with absorbance and excitation and fluorescence measurements, respectively) in the pH range from 4 to 10: (A) absorption spectra ($pK_a = 7.09 \pm 0.12$), (B) fluorescence spectra ($pK_a = 7.24 \pm 0.06$), (C) excitation spectra ($pK_a = 7.16 \pm 0.04$), and (D) the dual-excitation ratiometric response (Y_{400}/Y_{450}) with the linear fitting to changing the pH value (from 6.6 to 8.2), monitored at 472 nm.

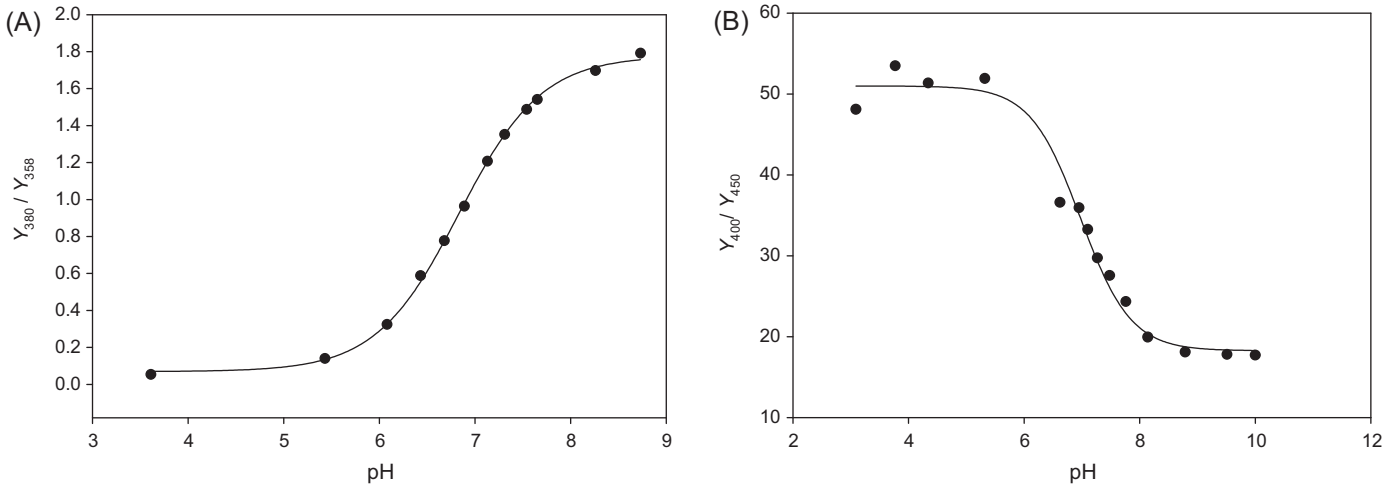

Fig. 8. The radiometric response as a function of pH (from 4 to 10) obtained from the measured excitation intensities ($Y_{\lambda 1}/Y_{\lambda 2}$) monitored at 452 nm and 472 nm in the emission spectrum of (A) **TLM** and (B) **DMPT**, respectively. The data fitted to the sigmoidal equation (4), see Section 2, gave pK_a values of 6.8 and 7.2 for **TLM** and **DMPT**, respectively, in pure water.

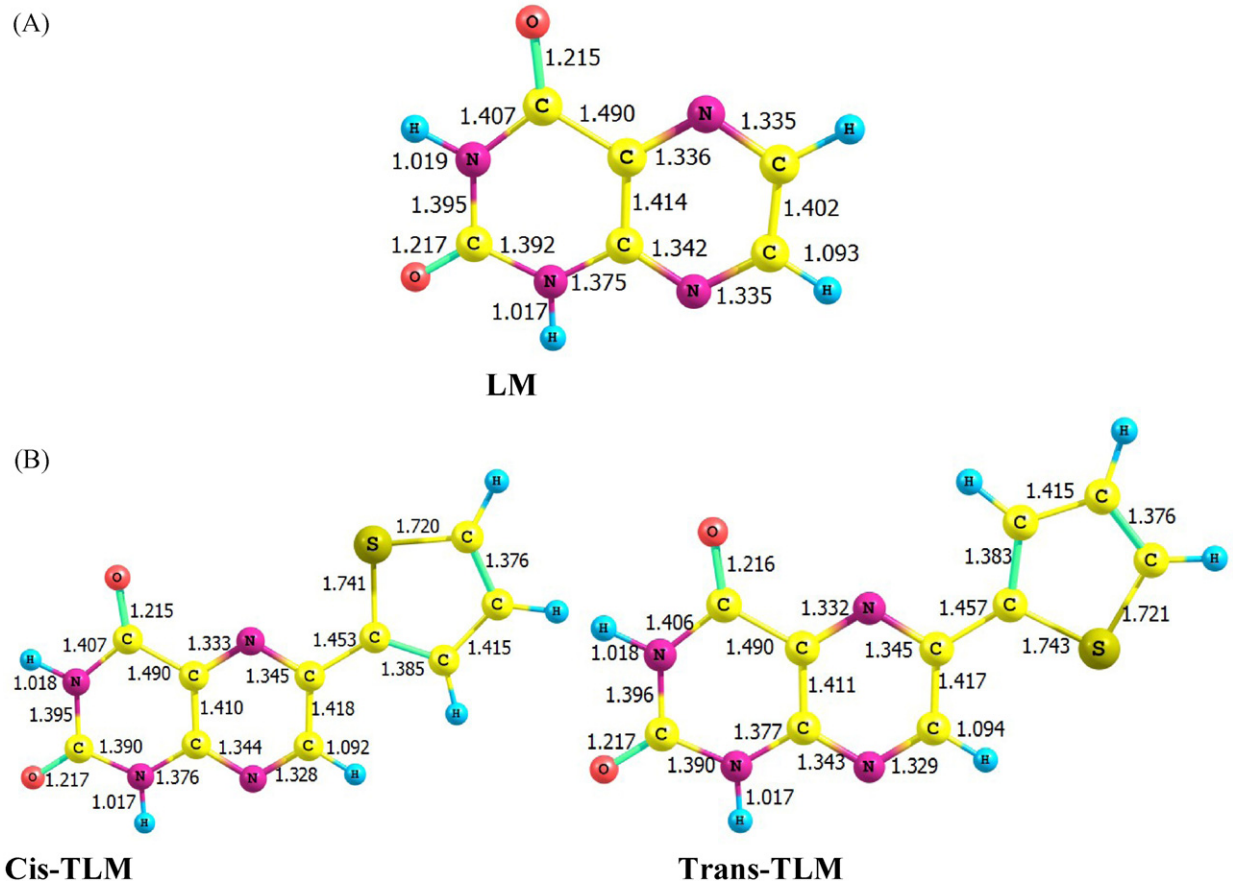

Fig. 9. The energy-minimized conformations of **LM** and **TLM**; bond lengths in Å.

analysis, failed to reveal any significant differences between the parent and substituted compounds. An alternative approach is to examine the energy of the HOMO of the conjugate base: The HOMO energy of a base is often a good indication of gas phase basicity and correspondingly, gas phase acidity for conjugate species. Correlations between HOMO energy and pK_a values have also been derived for mono- and bicyclic azines [61]. The HOMO energies of the conjugate bases of **LM**, **TLM**, **PT** and **DMPT** are given in Table 2. In each case the HOMO of the parent compound (**LM** or **PT**) is calculated to be higher in energy than the substituted species (**TLM** and **DMPT** respectively), consistent with the observed shifts in acidity. To investigate the effects of the individual substituents added to **PT**, calculations were also performed on the species **MPT** and **DPT**. The calculated HOMO energies of the conjugate bases of each species show additive behavior, with each added substituent lowering the energy of the HOMO and subsequently lowering the basicity of the conjugate base (enhancing acidity of the neutral compound).

3.4. Implication for applications

There have been several attempts in literature to tailor the design of new fluorescent dyes for having a pK_a values near-neutral pH in a rational way. Examples include, just to name a few, introducing electron-withdrawing group to fluoresceins-based dyes [23], incorporating a steric group on the nitrogen atom of the amide moiety on rhodamines-based dyes [26], as well as removal of hydroxylsulfonylbutyl motif on cyanine-based dyes [25]. We present herein an easy route to design a fluorescent pH sensor with a pK_a near 7. The synthesized pteridine dyes are produced via a facile, standard condensation reactions from natural starting materials (toxicity study in mice of **TLM** is also under investigation). As described in Section 2, the preparation is based on simple dehydration steps, while the design is based on the idea of inserting a stabilizing group for the formed anions to tune the pK_a value near-neutral pH. Moreover, the well-defined structure of the new dyes enabled us to introduce a specific functionality at the amine site of the pterin group (e.g., morpholine) that should enhance the cell retention and imaging, while slightly affecting (see theoretical results) the pK_a values of the dyes near physiological pH value.

Compared to those previously employed pH fluorescent indicators, the water-soluble, biologically relevant pteridine dyes that are presented in this work should have useful applications in monitoring pH changes inside living cells because of several attributes in addition to the synthetic prospective mentioned above, despites that additional studies are yet to be conducted and demonstrated for real biological applications of the synthesized compounds, including: photostability controls, quenching of their fluorescence by organic and inorganic compounds and study of the stability in biological media. First, the dyes show dual-excitation dependence on pH, which enables the ratio between the two signals to be nicely calibrated with the pH values. The ratiometric analysis is advantageous being independent of the total concentration of the dye, fluctuations of the source intensity, sensitivity of the instrument since both signals come from the dye under exactly the same instrumental conditions. Second, the dyes possess near-physiological pK_a values that are not sensitive to ionic strengths (data not shown). Interestingly, the absorption and fluorescence profile of **DMPT** were almost unchanged (decreased by only ~1–2%) with the addition of ~10 equivalents of any of the following metal ions salts (Cd^{2+}, Pd^{2+}, Mo^{2+}, Pt^{2+}, Rh^{3+}, Hg^{2+}, Hg^{+}, Co^{2+}, Fe^{2+}, Cu^{2+}, Ba^{2+}, Ag^{+}, Pb^{2+},

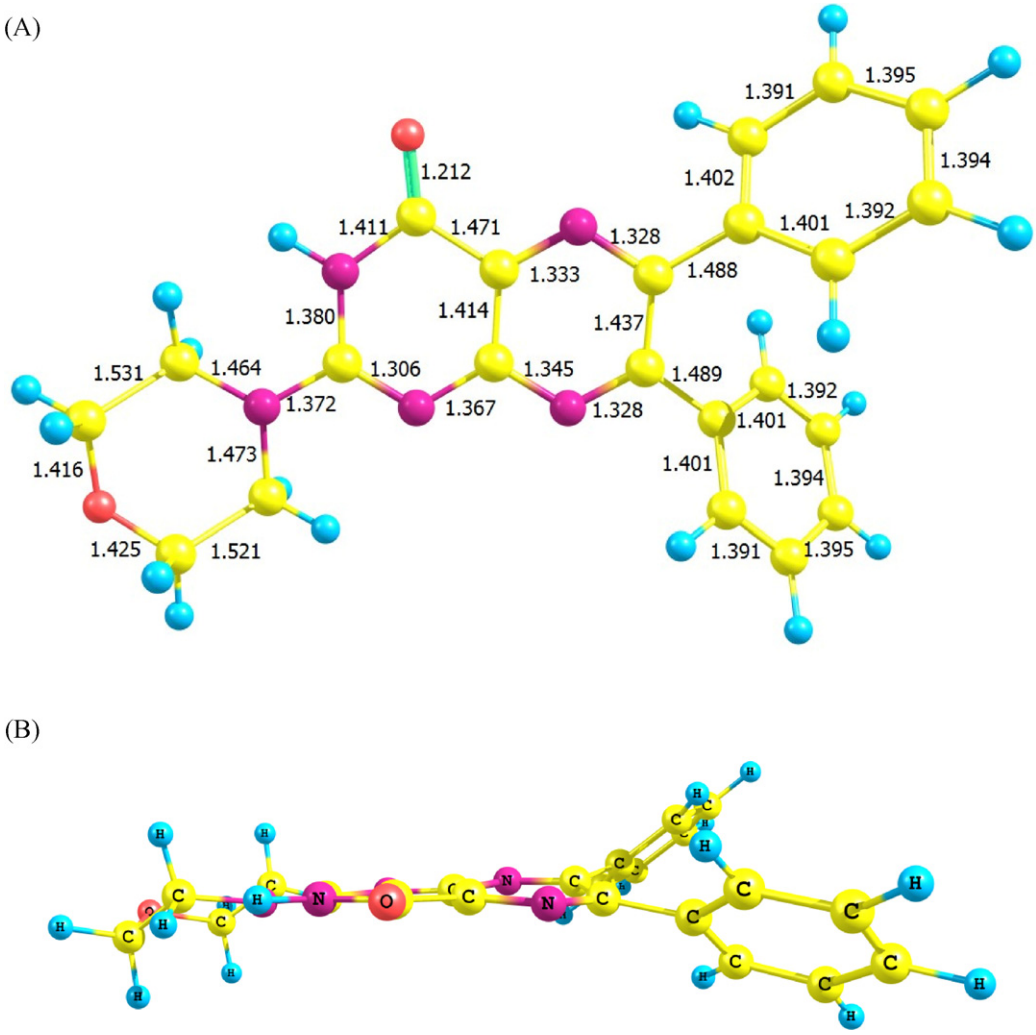

Fig. 10. The energy-minimized conformations of **DMPT**; bond lengths in Å.

Cs^+, Ni^{2+}, Cr^{3+}, Zn^{2+}, K^+, Na^+, Mg^{2+}, Ca^{2+}, Li^+, and Al^{3+}). Third, the new dyes exhibited high photostability in water as compared to **C450** (factor of 2, see Fig. S1 in the Supporting Information). Fourth, they showed reasonable quantum yield (0.1 in highly viscous glycol), and showed high absorption strengths. More importantly, **DMPT** dyes exhibited blue-to-cyan pH-dependent color change in their emission in water that can be visibly detected (see Fig. 11). Such a turn-on signal has an advantage over fluorescent quenching probes, which could provide false positive data by other fluorescent quenchers in real samples. Also, fluorescence quenching response often leads to a low-signal-to-noise ratio. Fifth, the dyes have considerable solubility in pure water (ca. ~1 mM at pH ~ 1 and pH ~ 12 for **TLM** and **DMPT**, respectively).

In particular, the facile synthesis of the dyes in this work gives them a special advantage as the preparation of pH indicators are known to be difficult [8]. Consequently, the present paper

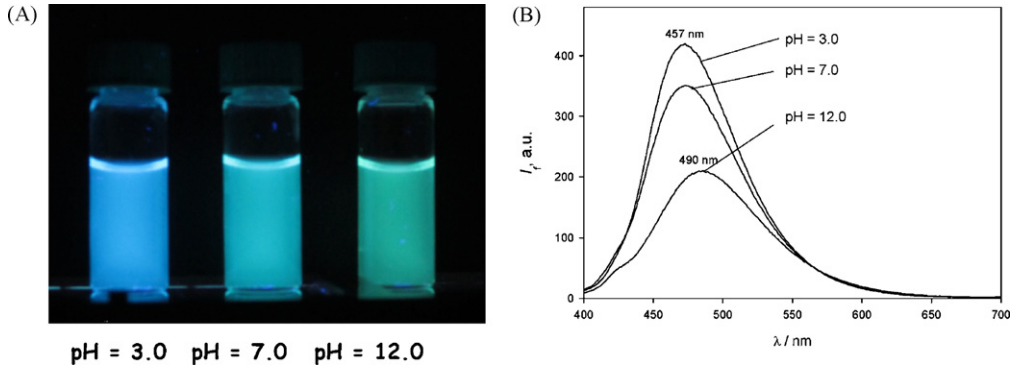

Fig. 11. The variation in the fluorescence spectra of **DMPT** in aqueous solution produced a gradual change in the emission color from blue to cyan that is visible to human eye: (A) real image; (B) the measured fluorescence profiles. (For interpretation of the references to color in this figure legend, the reader is referred to the web version of the article.)

could be incorporated into an organic/physical laboratory course to help undergraduate students explore the topic of fluorescent sensors.

4. Conclusions

In summary, new pteridine-based pH sensors (**TLM** and **DMPT**) were designed and easily synthesized, which are especially useful for application near-neutral pH (cf. pK_a of 7.2 for **DMPT**). The systematic tuning of the pK_a values by incorporating stabilizing groups on the pteridine platform for the conjugate bases was demonstrated experimentally and theoretically. Calculation of pK_a values using DFT methods and continuum solvent models failed to give values consistent with experiment. However, calculated orbital energies and gas phase acidities both indicate that the compounds **TLM** and **DMPT** are inherently more acidic than the parent species **LM** and **PT**, respectively. As a future outlook, the work offers newly designed pteridine-based pH sensors that should be suitable for monitoring pH variations inside the living cells via a fluorescence turn-on imaging.

Acknowledgments

N.S. would like to acknowledge the Office of Research Support and Sponsored Projects (RSSP) at the United Arab Emirates University for their financial support of this project under grant number 21S041 within the framework of National Research Foundation funding program (NRF). G.S. and A.A. gratefully acknowledge financial support from the Natural Sciences and Engineering Research Council of Canada (NSERC).

Appendix A. Supplementary data

Supplementary data associated with this article can be found, in the online version, at http://dx.doi.org/10.1016/j.jphotochem.2012.08.002.

References

[1] B. Valeur, Molecular Fluorescence: Principles and Applications, Wiley-VCH, New York/Heidelberg, 2002.
[2] J.R. Lakowicz, Topics in Fluorescence Spectroscopy, 2nd ed., Kluwer Academic/Plenum, New York/London, 1994.
[3] R.N. Dsouza, U. Pischel, W.M. Nau, Fluorescent dyes and their supramolecular host/guest complexes with macrocycles in aqueous Solution, Chemical Reviews 111 (2011) 7941–7980.
[4] H. Li, L. Cai, Z. Chen, Coumarin-derived fluorescent chemosensors, in: W. Wang (Ed.), Advances in Chemical Sensors, Intech, Rijeka, Croatia, 2011, pp. 121–150.
[5] V.M. Mirsky, A.K. Yatsimirsky, Quantitative affinity data on selected artificial receptor, in: V.M. Mirsky, A.K. Yatsimirsky (Eds.), Artificial Receptors for Chemical Sensors, Wiley-VCH, Weinheim, 2011, pp. 439–460.
[6] H.N. Kim, W.X. Ren, J.S. Kim, J. Yoon, Fluorescent and colorimetric sensors for detection of lead, cadmium, and mercury ions, Chemical Society Reviews 41 (2012) 3210–3244.
[7] E.M. Nolan, S.J. Lippard, Tools and tactics for the optical detection of mercuric ion, Chemical Reviews 108 (2008) 3443–3480.
[8] J. Han, K. Burgess, Fluorescent indicators for intracellular pH, Chemical Reviews 110 (2010) 2709–2728.
[9] D. Gust, J. Andreasson, U. Pischel, T.A. Moore, A.L. Moore, Data and signal processing using photochromic molecules, Chemical Communications 48 (2012) 1947–1957.
[10] R. Karoui, C. Blecker, Fluorescence spectroscopy measurement for quality assessment of food systems—a review, Food and Bioprocess Technology 4 (2011) 364–386.
[11] K. Virkler, I.K. Lednev, Analysis of body fluids for forensic purposes: from laboratory testing to non-destructive rapid confirmatory identification at a crime scene, Forensic Science International 188 (2009) 1–17.
[12] D. Aigner, S.M. Borisov, I. Klimant, New fluorescent perylene bisimide indicators—a platform for broadband pH optodes, Analytical and Bioanalytical Chemistry 400 (2011) 2475–2485.
[13] I. Grabchev, S. Guittonneau, Sensors for detecting metal ions and protons based on new green fluorescent poly (amidoamine) dendrimers peripherally modified with 1,8-naphthalimides, Journal of Photochemistry and Photobiology A 179 (2006) 28–34.
[14] Y. Xiong, Y. Huang, Z. Ye, Y. Guan, Flow injection small-volume fiber-optic pH sensor based on evanescent wave excitation and fluorescence determination, Journal of Fluorescence 21 (2011) 1137–1142.
[15] C.-W. Lee, C. Takagi, T. Truong, Y.-C. Chen, A. Ostafin, Luminescent Au nanoparticles with a pH-responsive nanoparticle-supported molecular brush, The Journal of Physical Chemistry C 114 (2010) 12459–12468.
[16] N. Saleh, Y.A. Al-Soud, L. Al-Kaabi, I. Ghosh, W.M. Nau, A coumarin-based fluorescent PET sensor utilizing supramolecular pK_a shifts, Tetrahedron Letters 52 (2011) 5249–5254.
[17] N. Saleh, Y.A. Al-Soud, W.M. Nau, Novel fluorescent pH sensor based on coumarin with piperazine and imidazole substituents, Spectrochimica Acta Part A 71 (2008) 818–822.
[18] D. Staneva, I. Grabchev, J.-P. Soumillion, V. Bojinov, A new fluorosensor based on bis-1,8-naphthalimide for metal cations and protons, Journal of Photochemistry and Photobiology A 189 (2007) 192–197.
[19] N.V. Marinova, N.I. Georgiev, V.B. Bojinov, Design, synthesis and pH sensing properties of novel 1,8-naphtalimide-based bichromophoric system, Journal of Photochemistry and Photobiology A 222 (2011) 132–140.
[20] J. Xie, Y. Chen, W. Yang, D. Xu, K. Zhang, Water soluble 1,8-naphthalimide fluorescent pH probes and their application to bioimagings, Journal of Photochemistry and Photobiology A 223 (2011) 111–118.
[21] L. Yuan, W. Lin, Z. Cao, J. Wang, B. Chen, Development of FRET-based dual-excitation ratiometric fluorescent pH probes and their photocaged derivatives, Chemistry: A European Journal 18 (2012) 1247–1255.
[22] Y. Xu, Y. Liu, X. Qian, Novel cyanine dyes as fluorescent pH sensors: PET, ICT mechanism or resonance effect? Journal of Photochemistry and Photobiology A 190 (2007) 1–8.
[23] J.X. Liu, Z.J. Diwu, D.H. Klaubert, Fluorescent molecular probes—III. 2′,7′-Bis-(3-carboxypropyl)-5-(and-6)-carboxyfluorescein (BCPCF): a new polar dual-excitation and dual-emission pH indicator with a pK_a of 7.0, Bioorganic & Medicinal Chemistry Letters 7 (1997) 3069–3072.
[24] J.X. Liu, Z.J. Diwu, W.Y. Leung, Synthesis and photophysical properties of new fluorinated benzo c xanthene dyes as intracellular pH indicators, Bioorganic & Medicinal Chemistry Letters 11 (2001) 2903–2905.
[25] Z.R. Zhang, S. Achilefu, Design, synthesis and evaluation of near-infrared fluorescent pH indicators in a physiologically relevant range, Chemical Communications (2005) 5887–5889.
[26] L. Yuan, W. Lin, Y. Feng, A rational approach to tuning the pK_a values of rhodamines for living cell fluorescence imaging, Organic & Biomolecular Chemistry 9 (2011) 1723–1726.
[27] N. Saleh, A.M.M. Rawashdeh, Y.A. Yousef, Y.A. Al-Soud, Structural characterization of new Cd^{2+} fluorescent sensor based on lumazine ligand: AM1 and ab initio studies, Spectrochimica Acta Part A 68 (2007) 728–733.
[28] N. Saleh, Luminescent sensor for Cd^{2+}, Hg^{2+} and Ag^{+} in water based on a sulphur-containing receptor: quantitative binding-softness relationship, Luminescence 24 (2009) 30–34.
[29] H. Matter, P. Kotsonis, Biology and chemistry of the inhibition of nitric oxide synthases by pteridine-derivatives as therapeutic agents, Medicinal Research Reviews 24 (2004) 662–684.
[30] P.F. Heelis, S.T. Kim, T. Okamura, A. Sancar, The photo repair of pyrimidine dimers by DNA photolyase and model systems, Journal of Photochemistry and Photobiology B: Biology 17 (1993) 219–228.
[31] R.C. Fuller, G.W. Kidder, N.A. Nugent, V.C. Dewey, RigopoulN., Association and activities of pteridines in photosynthetic systems, Photochemistry and Photobiology 14 (1971) 359–361.
[32] A.H. Thomas, C. Lorente, A.L. Capparelli, M.R. Pokhrel, A.M. Braun, E. Oliveros, Fluorescence of pterin, 6-formylpterin, 6-carboxypterin and folic acid in aqueous solution: pH effects, Photochemical & Photobiological Sciences 1 (2002) 421–426.
[33] M.P. Denofrio, A.H. Thomas, A.M. Braun, E. Oliveros, C. Lorente, Photochemical and photophysical properties of lumazine in aqueous solutions, Journal of Photochemistry and Photobiology A 200 (2008) 282–286.
[34] F.M. Cabrerizo, G. Petroselli, C. Lorente, A.L. Capparelli, A.H. Thomas, A.M. Braun, E. Oliveros, Substituent effects on the photophysical properties of pterin derivatives in acidic and alkaline aqueous solutions, Photochemistry and Photobiology 81 (2005) 1234–1240.
[35] M.S. Kritsky, T.A. Lyudnikova, E.A. Mironov, I.V. Moskaleva, The UV radiation-driven reduction of pterins in aqueous solution, Journal of Photochemistry and Photobiology B: Biology 39 (1997) 43–48.
[36] G. Suarez, F.M. Cabrerizo, C. Lorente, A.H. Thomas, A.L. Capparelli, Study of the photolysis of 6-carboxypterin in acid and alkaline aqueous solutions, Journal of Photochemistry and Photobiology A 132 (2000) 53–57.
[37] Y. Aoki, N. Umezawa, Y. Asano, K. Hatano, Y. Yano, N. Kato, T. Higuchi, A versatile strategy for the synthesis of crown ether-bearing heterocycles: discovery of calcium-selective fluoroionophore, Bioorganic & Medicinal Chemistry 15 (2007) 7108–7115.
[38] M.S. Han, D.H. Kim, Readily available fluorescence probes for zinc ion in aqueous solution of neutral pH, Supramolecular Chemistry 15 (2003) 59–64.
[39] A. Albert, Quantitative studies of the avidity of naturally occurring substances for trace metals. 3. Pteridines, riboflavin and purines, The Biochemical Journal 54 (1953) 646–654.
[40] A. Albert, D.J. Brown, G. Cheeseman, 103. Pteridine studies. Part I. Pteridine, and 2- and 4-amino- and 2- and 4-hydroxy-pteridines, Journal of the Chemical Society (1951) 474–485.

[41] C. Hemann, P. Ilich, R. Hille, Vibrational spectra of lumazine in water at pH 2–13: ab initio calculation and FTIR/Raman spectra, The Journal of Physical Chemistry B 107 (2003) 2139–2155.
[42] M.D. Davis, J.S. Olson, G. Palmer, The reaction of xanthine oxidase with lumazine. Characterization of the reductive half-reaction, The Journal of Biological Chemistry 259 (1984) 3526–3533.
[43] W. Pfleiderer, Pteridine. 1. Uber 2.4-dioxo-tetrahydropteridine, Chemische Berichte-Recueil 90 (1957) 2582–2587.
[44] G. Jones, M.A. Rahman, Fluorescence properties of coumarin laser-dyes in aqueous polymer media—chromophore isolation in ploy(methacrylic acid) hypercoils, The Journal of Physical Chemistry 98 (1994) 13028–13037.
[45] J. Wu, L. Isaacs, Cucurbit[7]uril complexation drives thermal trans-cis-azobenzene isomerization and enables colorimetric amine detection, Chemistry: A European Journal 15 (2009) 11675–11680.
[46] J. Adcock, C.L. Gibson, J.K. Huggan, C.J. Suckling, Diversity oriented synthesis: substitution at C5 in unreactive pyrimidines by Claisen rearrangement and reactivity in nucleophilic substitution at C2 and C4 in pteridines and pyrido[2,3-d]pyrimidines, Tetrahedron 67 (2011) 3226–3237.
[47] M.J. Frisch, G.W. Trucks, H.B. Schlegel, G.E. Scuseria, M.A. Robb, J.R. Cheeseman, J.A. Montgomery, T. Vreven, K.N. Kudin, J.C. Burant, J.M. Millam, S.S. Iyengar, J. Tomasi, V. Barone, B. Mennucci, M. Cossi, G. Scalmani, N. Rega, G.A. Petersson, H. Nakatsuji, M. Hada, M. Ehara, K. Toyota, R. Fukuda, J. Hasegawa, M. Ishida, T. Nakajima, Y. Honda, O. Kitao, H. Nakai, M. Klene, X. Li, J.E. Knox, H.P. Hratchian, J.B. Cross, V. Bakken, C. Adamo, J. Jaramillo, R. Gomperts, R.E. Stratmann, O. Yazyev, A.J. Austin, R. Cammi, C. Pomelli, J.W. Ochterski, P.Y. Ayala, K. Morokuma, G.A. Voth, P. Salvador, J.J. Dannenberg, V.G. Zakrzewski, S. Dapprich, A.D. Daniels, M.C. Strain, O. Farkas, D.K. Malick, A.D. Rabuck, K. Raghavachari, J.B. Foresman, J.V. Ortiz, Q. Cui, A.G. Baboul, S. Clifford, J. Cioslowski, B.B. Stefanov, G. Liu, A. Liashenko, P. Piskorz, I. Komaromi, R.L. Martin, D.J. Fox, T. Keith, M.A. Al-Laham, C.Y. Peng, A. Nanayakkara, M. Challacombe, P.M.W. Gill, B. Johnson, W. Chen, M.W. Wong, C. Gonzalez, J.A. Pople, Gaussian 03W, Revision E.01, CT Gaussian Inc., Wallingford, 2004.
[48] A.D. Becke, Density-functional thermochemistry. III. The role of exact exchange, The Journal of Chemical Physics 98 (1993) 5648–5652.
[49] M. Cossi, N. Rega, G. Scalmani, V. Barone, Energies, structures, and electronic properties of molecules in solution with the C-PCM solvation model, Journal of Computational Chemistry 24 (2003) 669–681.
[50] M.J. Kamlet, J.L.M. Abboud, M.H. Abraham, R.W. Taft, Linear solvation energy relationships. 23. A comprehensive collection of the solvatochromic parameters, p^*, a and b, and some methods for simplifying the generalized solvatochromic equation, The Journal of Organic Chemistry 48 (1983) 2877–2887.
[51] K. Hirakawa, H. Suzuki, S. Oikawa, S. Kawanishi, Sequence-specific DNA damage induced by ultraviolet A-irradiated folic acid via its photolysis product, Archives of Biochemistry and Biophysics 410 (2003) 261–268.
[52] C. Lorente, A.L. Capparelli, A.H. Thomas, A.M. Braun, E. Oliveros, Quenching of the fluorescence of pterin derivatives by anions, Photochemical & Photobiological Sciences 3 (2004) 167–173.
[53] G. Petroselli, M.L. Dantola, F.M. Cabrerizo, C. Lorente, A.M. Braun, E. Oliveros, A.H. Thomas, Quenching of the fluorescence of aromatic pterins by deoxynucleotides, The Journal of Physical Chemistry A 113 (2009) 1794–1799.
[54] R. Klein, I. Tatischeff, Tautomerism and fluorescence of lumazine, Photochemistry and Photobiology 45 (1987) 55–65.
[55] K.N. Rogstad, Y.H. Jang, L.C. Sowers, W.A. Goddard III, First principles calculations of the pK_a values and tautomers of isoguanine and xanthine, Chemical Research in Toxicology 16 (2003) 1455–1462.
[56] Y.H. Jang, W.A. Goddard Iii, K.T. Noyes, L.C. Sowers, S. Hwang, D.S. Chung, pK_a values of guanine in water: density functional theory calculations combined with Poisson-Boltzmann continuum-solvation model, The Journal of Physical Chemistry B 107 (2003) 344–357.
[57] M.J.S. Dewar, H.N. Schmeising, A re-evaluation of conjugation and hyperconjugation: the effects of changes in hybridisation on carbon bonds, Tetrahedron 5 (1959) 166–178.
[58] J. Crugeiras, A. Ríos, H. Maskill, DFT and AIM study of the protonation of nitrous acid and the pK_a of nitrous acidium ion, The Journal of Physical Chemistry A 115 (2011) 12357–12363.
[59] M.D. Liptak, G.C. Shields, Accurate pK_a calculations for carboxylic acids using Complete Basis Set and Gaussian-n models combined with CPCM continuum solvation methods, Journal of the American Chemical Society 123 (2001) 7314–7319.
[60] C.P. Kelly, C.J. Cramer, D.G. Truhlar, Aqueous solvation free energies of ions and ion-water clusters based on an accurate value for the absolute aqueous solvation free energy of the proton, The Journal of Physical Chemistry B 110 (2006) 16066–16081.
[61] H.J. Soscún Machado, A. Hinchliffe, Relationships between the HOMO energies and pK_a values in monocyclic and bicyclic azines, Journal of Molecular Structure 339 (1995) 255–258.
[62] W.M. Haynes, D.R. Lide, CRC Handbook of Chemistry and Physics: A Ready-reference Book of Chemical and Physical Data, CRC, Boca Raton, 2010.